Complex self-propelled rings: a minimal model for cell motility. Supporting Information

I. FRICTION

In order to characterize the dynamics of self-propelled rods circling inside stationary rings, we calculate an effective friction that the rods feel as they slide along the ring,

$$\mu = \left\langle \frac{\mathbf{F}_\mathrm{P} \cdot \mathbf{e}_\mathrm{t}}{\mathbf{v}_\mathrm{r} \cdot \mathbf{e}_\mathrm{t}} \right\rangle_{N_\mathrm{r},t}, \tag{1}$$

where $\mathbf{e}_\mathrm{t}$ is the unit vector along the tangential direction of the ring, $\mathbf{F}_\mathrm{P}$ is the rod propulsion force, and $\mathbf{v}_\mathrm{r}$ is the rod velocity.

Figure S1 shows the normalized friction coefficient, $(\mu - \mu_0)/\mu_0$, versus the inverse overlap, ζ, for $N_\mathrm{r} = 1$ and 6 and $E_\mathrm{r}/k_\mathrm{B}T = 10$. μ_0 is the effective friction for rods sliding along a continuous ring. The normalized effective friction coefficient $(\mu - \mu_0)/\mu_0$ versus ζ can be fitted using

$$\frac{\mu - \mu_0}{\mu_0} = a\zeta^b, \tag{2}$$

where a and b are fit parameters, see Tab. S1.

For the studied systems, the only parameters that play a role in the effective friction are N_r and ζ, see Fig. S1. Our measured friction coefficients do not depend on Pe and for small numbers of rods and no clustering, also N_r does affect the friction coefficient significantly. Therefore, for small rod densities where the rods do not cluster, the friction between the ring and rods only depends on ζ. The values for a and b increase as N_r increases, both for attached and non-attached rods.

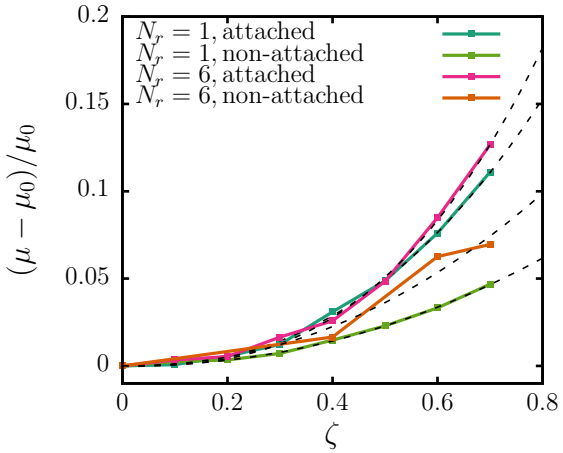

FIG. S1: Normalized effective friction coefficient, $(\mu - \mu_0)/\mu_0$, versus inverse overlap, ζ, for attached and non-attached rods systems with varying N_r. The dashed lines are fits using Eq. (2).

Types of rods	N_r	a	b
Attached	1	0.3	2.4
	6	0.3	2.7
Non-Attached	1	0.1	2.1
	6	0.2	2.1

TABLE S1: Fit parameters for the systems shown in Fig. S1.

II. STATIONARY RING: ROD DYNAMICS AND ROD ALIGNMENT

The dynamics of most of the rod systems can be characterized effectively using the orientation autocorrelation function

$$C(t) = \langle \mathbf{l}_i(t' + t) \cdot \mathbf{l}_i(t') \rangle \tag{3}$$

for lag time t, where $\mathbf{l}_i(t')$ is the orientation vector of rod i at time t'. For periodical systems, the period of the circular motion of the rods inside the ring is

$$T = \frac{2\pi R_\mathrm{m}\mu}{\mathbf{F}_\mathrm{r} \cdot \mathbf{e}_\mathrm{t}}, \tag{4}$$

where R_m is the ring radius, $\mathbf{F}_\mathrm{r}$ is the rod propulsion force, $\mathbf{e}_\mathrm{t}$ is the unit vector along the tangential direction of the ring, and μ is the effective friction between rods and ring. The period T can also be extracted from the orientation autocorrelation functions, see Fig. S2.

A. NON-ATTACHED AND ATTACHED-PUSHING RODS

Figures S2A and S2B show orientation autocorrelation functions for circling and for clustering of attached-pushing rods, respectively; figures S2C and S2D show the analogous autocorrelation functions for non-attached rods. The error bars are calculated using the standard deviations for the averages over both time and rods.

For circling rods, the orientation autocorrelation function oscillates with a constant period and its amplitude decays with time, see Figs. S2A and S2C. The period for non-attached rods, Fig. S2C, is roughly the same than that for attached-pushing rods, see Tab. S2. Thus, the attachment of the rods to the ring does not affect the rods tangential velocity, but it does affect the speed at which rods decorrelate, see Tab. S2. The amplitudes of the orientation correlation functions for non-attached rods decay more quickly than for attached-pushing rods. This difference in the speed of the decorrelation is due to the fact that non-attached rods slide and jump along the ring while attached rods can only slide. For systems that do

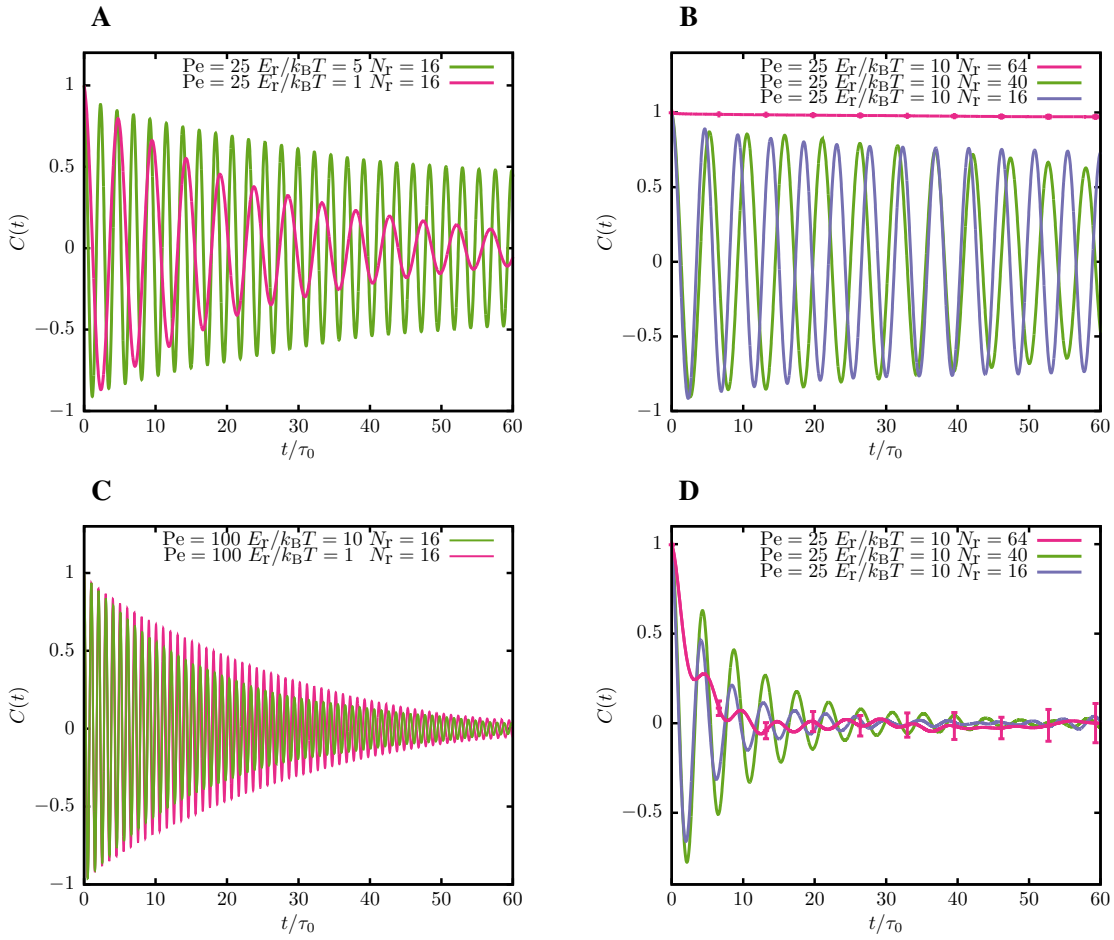

FIG. S2: Rod orientation autocorrelation function, $C(t)$, versus lag time, t. A) Attached-pushing rod systems with $N_r = 16$ and Pe = 25, B) attached-pushing rod systems with Pe = 25 and $E_r/k_BT = 10$, C) non-attached rod systems with $N_r = 16$ and Pe = 100, and D) Non-attached rod systems with Pe = 25 and $E_r/k_BT = 10$.

N_r	Pe	E_r/k_BT	T_{as}	T_{ar}	T_{ns}	T_{nr}	τ_{as}	τ_{ns}	τ_{nr}
16	25	1	4.79	4.91	3.78	3.95	23.46	4.53	7.38
		10	4.62	4.72	4.14	4.29	-	5.52	8.18
	100	1	1.07	1.12	1.01	-	-	24.76	-
		10	1.12	1.21	1.02	1.06	-	17.1	23.6
64	25	1	5.51	5.61	4.07	4.15	10.28	5.53	7.84
		10	-	-	4.69	-	-	2.57	5.27
	100	1	1.13	1.15	1.04	1.08	-	15.49	20.37

TABLE S2: Time periods extracted from the autocorrelation functions for rod orientation for systems with attached-pushing and non-attached rods with Pe = 25 and 100, $E_r/k_BT = 1$ and 10, and $N_r = 16$ and 64. The periods T_{as} and T_{ar} are for attached-pushing rods in smooth and rough rings, respectively. The periods T_{ns} and T_{nr} are for non-attached rods in smooth and rough rings, respectively. The relaxation time τ_{as} characterizes the decorrelation for attached-pushing rods in a smooth ring, τ_{ns} for non-attached rods in a smooth ring, and τ_{nr} for non-attached rods in a rough ring. All time-related quantities are given in units of the single-rod relaxation time τ_0. Systems for that no period is given do not show periodic motion.

not show periodic motion stationary clusters are observed for $E_r/k_BT = 10$ and Pe = 25 and $N_r = 64$, see Fig. S2B. Dynamic clusters are observed for $E_r/k_BT = 10$, Pe = 25 and $N_r = 64$ for non-attached rods, see Fig. S2D. While stationary clusters lead to a very slow decay of the orientation autocorrelation function, dynamic clusters show a rapid exponential decay overlaid with a sinusoidal dependence.

The orientation autocorrelation function for all circling rod systems, both unidirectional and bidirectional, and

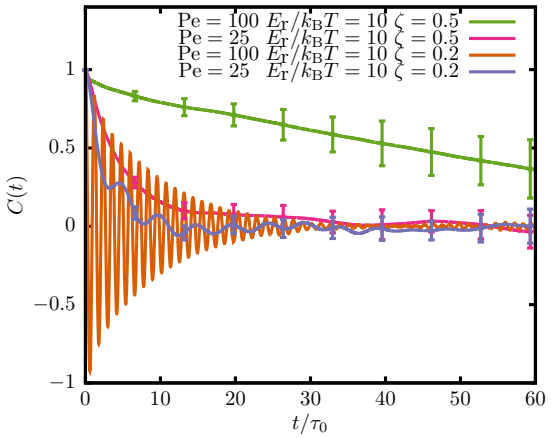

FIG. S3: Orientation autocorrelation function of non-attached rods, $C(t)$, versus lag time, t. Comparison between systems with $N_r = 64$, Pe = 25 and 100, and varying ζ.

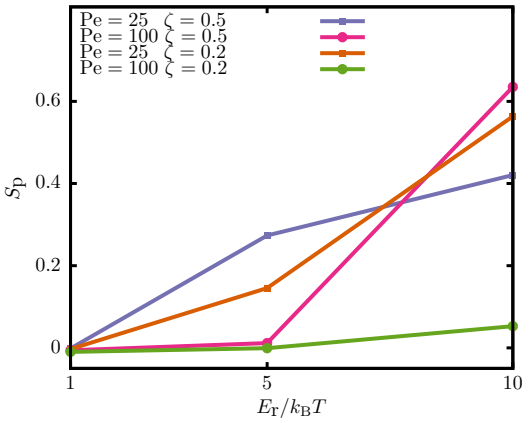

FIG. S4: Polar order parameter, S_P, versus energy barrier, E_r, for non-attached-rod systems with $N_r = 64$ inside a ring with $\zeta = 0.5$.

for the dynamic-cluster systems shown in Fig. S2, have been fitted using

$$C(t) = e^{(-t/\tau)} \cos(t/T), \tag{5}$$

where t is the lag time, τ is the relaxation time, and T is the period. The exponential function accounts for the relaxation of the amplitude, and the sinusoidal function accounts for the periodicity of the circling. The results from these fits are shown in Tab. S2. For some of the systems with attached-pushing rods no periodic motion is observed, whereas non-attached rods always show periodic motion.

Although the period does not change with increasing roughness of the ring, some systems which show periodic motion for smooth rings, $\zeta = 0.2$, show no periodic motion for rough rings, $\zeta = 0.5$. Figure S3 shows orientation autocorrelation functions for systems with non-attached rods, $\zeta = 0.2$ and 0.5, and Pe = 25 and 100. For rods with Pe = 25 the systems transit from dynamic clusters towards more stationary clusters with increasing ζ. Therefore, autocorrelation functions for $\zeta = 0.5$ decay more slowly than for $\zeta = 0.2$; the relaxation times increase from $\tau_{ns} = 2.57\tau_0$ to $\tau_{nr} = 5.27\tau_0$, see Tab. S2. The dependence on the roughness of the rings is even more pronounced for systems with high Pe. For a smooth ring with $\zeta = 0.2$ and Pe = 100 a circling cluster is observed and the envelope of the oscillating autocorrelation function decays quickly. For a rough ring with $\zeta = 0.5$, the cluster is more stationary and a slow decay of the orientation autocorrelation function is observed.

The polar order parameter, S_P, defined in Eq. (8) in the main text, is also affected by ζ, see Fig. S4. For intermediate energy barrier, $E_r/k_BT = 5$, the rods transit from unidirectional circling to a cluster if ζ increases from 0.2 to 0.5. The cluster formation causes an increase of the polar order parameter. Once the rods are impenetrable, with $E_r/k_BT = 10$, the polar order parameters for rods inside smooth and rough rings are similar for systems with Pe = 100. For systems with Pe = 25 inside smooth rings, $\zeta = 0.2$, the rods circle, whereas inside rough rings $\zeta = 0.5$ the rods cluster.

E_r	N_r	Pe	a	b	c	τ_1/τ_0	τ_2/τ_0
0	-	25	0.254	0.743	0.003	0.464	14.551
		100	0.0563	0.906	0.036	0.069	27.41
k_BT	16	25	0.27	0.721	0.005	0.60	21.5
		100	0.051	0.887	0.061	0.0612	35.016
	64	25	0.1963	0.845	-0.041	0.50	44.0
		100	0.049	1.045	-0.0949	0.0934	102.800

TABLE S3: Fit parameters obtained using Eq. (6) for the data shown in Fig. S5.

B. ATTACHED-PULLING RODS

Figure S5 shows orientation autocorrelation functions for $N_r = 16$ and 40 interacting and non-interacting attached-pulling rods in smooth rings. The rod orientation decorrelates faster for lower rod density, smaller E_r, and lower Pe. We fit the orientation autocorrelation function for using

$$C(t) = ae^{-t/\tau_1} + be^{-t/\tau_2} + c, \tag{6}$$

where τ_1, and τ_2 are relaxation times. For non-interacting systems, $E_r = 0$, the decorrelation speed depends on Pe. For systems with Pe = 25, there are two degrees of freedom for the rods, the orientation of the rods and the position within the ring. For systems with Pe = 100 the rod tends to remain attached to the same bead of the ring throughout the simulation, thus there is effectively only one degree of freedom.

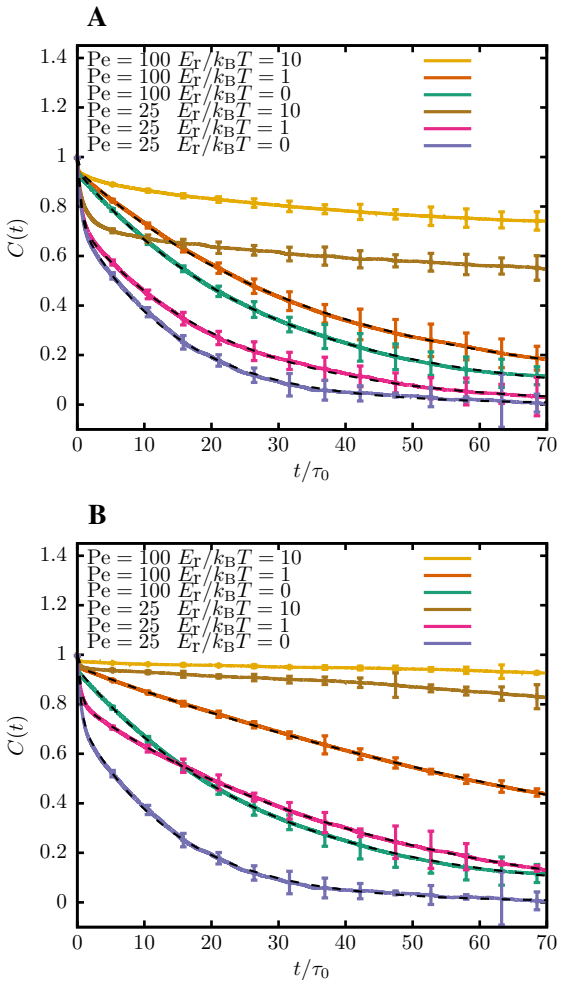

FIG. S5: Rod orientation autocorrelation, $C(t)$, versus lag time, t, for attached-pulling-rod systems . A) Attached-pulling rod systems with $N_r = 16$, and B) attached-pulling rod systems with $N_r = 64$. Continuous lines are simulation results; dashed lines are fits using Eq. (6). Error bars are calculated using the standard deviation of the average over time and rods for each system.

C. SUMMARY

In summary, there are four types of dynamics observed in our systems: unidirectional circling, bidirectional circling, circling clusters, and stationary clusters. The dynamics of non-attached rods and attached-pushing rods are similar, although the attachment reduces the velocity at which rods decorrelate, see Fig. S2 and Tab. S2. Attached-pulling rods decorrelate exponentially with time, see Fig. S5 and Tab. S3, where the decorrelation time depends on the energy barrier, E_r, the Peclet number, Pe, and the number of rods, N_r. As the effective friction between the rods and ring increases, the rods cluster more easily and both rod alignment and correlation time increase. These effects are more noticeable for non-attached rods, see Figs. S3 and S4.

MOVIES

Random-walk motion video: System with $N_r = 16$ attached-pushing rods, $E_r/k_BT = 1$, Pe = 100, $\xi = 0.2$, $\eta = 0.005 k_BT\tau_0/L_r$. The left part of the video shows the dynamics of the self-propelled rods inside the ring, the right part of the video shows the trajectory of the center of the ring. The attached-pushing rods circle bidirectionally, both clockwise and counterclockwise.

Persistent motion video: System with $N_r = 64$ attached-pulling rods, $E_r/k_BT = 1$, Pe = 25, $\xi = 0.2$, $\eta = 0.005 k_BT\tau_0/L_r$. The left part of the video shows the dynamics of the self-propelled rods inside the ring, the right part of the video shows the trajectory of the center of the ring. The attached-pulling rods form a loose cluster.

Circling motion: System with $N_r = 16$ attached-pushing and attached-pulling rods, $E_r/k_BT = 10$, Pe = 100, $\xi = 0.2$, $\eta = 0.005 k_BT\tau_0/L_r$. The left part of the video shows the dynamics of the self-propelled rods inside the ring, the right part of the video shows the trajectory of the center of the ring. The rods form a circling cluster which circles clockwise. All the attached-pushing rods, except for one which is out of the cluster, are on the left side of the cluster. This allows the attached-pushing rods to exert enough force to make the attached-pulling rods circle.

Run-and-circle motion: System with $N_r = 16$ attached-pushing and attached-pulling rods, $E_r/k_BT = 10$, Pe = 50, $\xi = 0.2$, $\eta = 0.005 k_BT\tau_0/L_r$. The left part of the video shows the dynamics of the self-propelled rods inside the ring, the right part of the video shows the trajectory of the center of the ring. During the circling part of the motion the rods form one cluster which circles counterclockwise. During the running part of the motion three of the pushing rods on the right side of the cluster de-attach from the cluster and circle in a clockwise direction. Once these three rods encounter the cluster the ring starts circling again.